Nature and Origin of Mineralizing Fluids in Hyperextensional Systems: The Case of Cretaceous Mg Metasomatism in the Pyrenees

Benoît Quesnel, Marie-Christine Boiron, Michel Cathelineau, Laurent Truche, Thomas Rigaudier, Gérard Bardoux, Pierre Agrinier, Michel de Saint Blanquat, Emmanuel Masini, Eric C. Gaucher

Hindawi
Geofluids
Volume 2019, Article ID 7213050, 18 pages
https://doi.org/10.1155/2019/7213050

Research Article

Nature and Origin of Mineralizing Fluids in Hyperextensional Systems: The Case of Cretaceous Mg Metasomatism in the Pyrenees

Benoît Quesnel,[1] Marie-Christine Boiron,[1] Michel Cathelineau,[1] Laurent Truche,[2] Thomas Rigaudier,[3] Gérard Bardoux,[4] Pierre Agrinier,[4] Michel de Saint Blanquat,[5] Emmanuel Masini,[6,7] and Eric C. Gaucher[6]

[1]*Université de Lorraine, CNRS, CREGU, GeoRessources, F-54000 Nancy, France*
[2]*Université Grenoble Alpes, CNRS, ISTerre, F-38000 Grenoble, France*
[3]*CRPG-CNRS, Université de Lorraine, UMR 7358, 54501 Vandoeuvre-lès-Nancy Cedex, France*
[4]*Institut de Physique du Globe de Paris, Sorbonne Paris Cité, Université Paris Diderot, UMR 7154 CNRS, F-75005 Paris, France*
[5]*Geosciences Environnement Toulouse (GET), OMP, CNRS, IRD, Université de Toulouse, 14 Avenue Edouard Belin, 31400 Toulouse, France*
[6]*Total, CSTJF, Avenue Larribau, F-64018 Pau, France*
[7]*M&U SAS, 3 Rue des Abattoirs, 38120 Saint-Egrève, France*

Correspondence should be addressed to Benoît Quesnel; benoit.quesnel.1@ulaval.ca

Received 17 January 2019; Revised 17 May 2019; Accepted 28 May 2019; Published 17 July 2019

Academic Editor: Fabien Magri

During the Albian, the hyperextension of the Pyrenean passive margin led to a hyperthinning of the continental crust and the subsequent subcontinental mantle exhumation. The giant Trimouns talc-chlorite deposit represents the most prominent occurrence of Albian metasomatism in the Pyrenees, with the occurrence of the largest talc deposit worldwide. Consequently, this deposit, which is located on a fault zone and a lithological contact, represents one of the major drains at the scale of the Pyrenees and one of the best geological targets in order to determine the origin(s) of the fluid(s) that circulated during this period. Talc-chlorite ore is characterized by the presence of brines trapped in dolomite, quartz, and calcite fluid inclusions in the vicinity of the talc-rich zone. Considered as being responsible for the formation of talc, these fluids may be interpreted in several ways: (i) primary brines expelled from Triassic evaporites, (ii) secondary brines produced through halite leaching by diagenetic/metamorphic fluids, and (iii) brines derived from seawater serpentinization of mantle rocks. Stable isotope analyses ($\delta^{13}C$, $\delta^{18}O$, δD, and $\delta^{37}Cl$) and Cl/Br ratio measurements in fluid inclusions and their host minerals were carried out in order to determine the origin of the fluid(s) involved in the formation of the ore deposit. The data are consistent with a primary brine origin for the mineralizing fluid, which could have been expelled from the Triassic levels. Other hypotheses have been tested, for example, the production of brines via the seawater concentration during serpentinization. The geochemical proxies used in this study provide equivocal results. The first hypothesis is by far the most realistic one considering the numerous occurrences of Trias formations nearby, their deformation during the extension, and the drainage of the expulsed brines as evidenced by the high-salinity fluid inclusions found all around the deposit. Alternatively, the exhumation of the mantle is considered as a major source of heat and stress that favored brine migration along the major shear zones. Our results fit well with brine circulation in a hyperextensional geodynamic context, which is related to the formation of the talc-chlorite ore, the thinning of the continental crust, and the exhumation of the subcontinental mantle, in accordance with recent works.

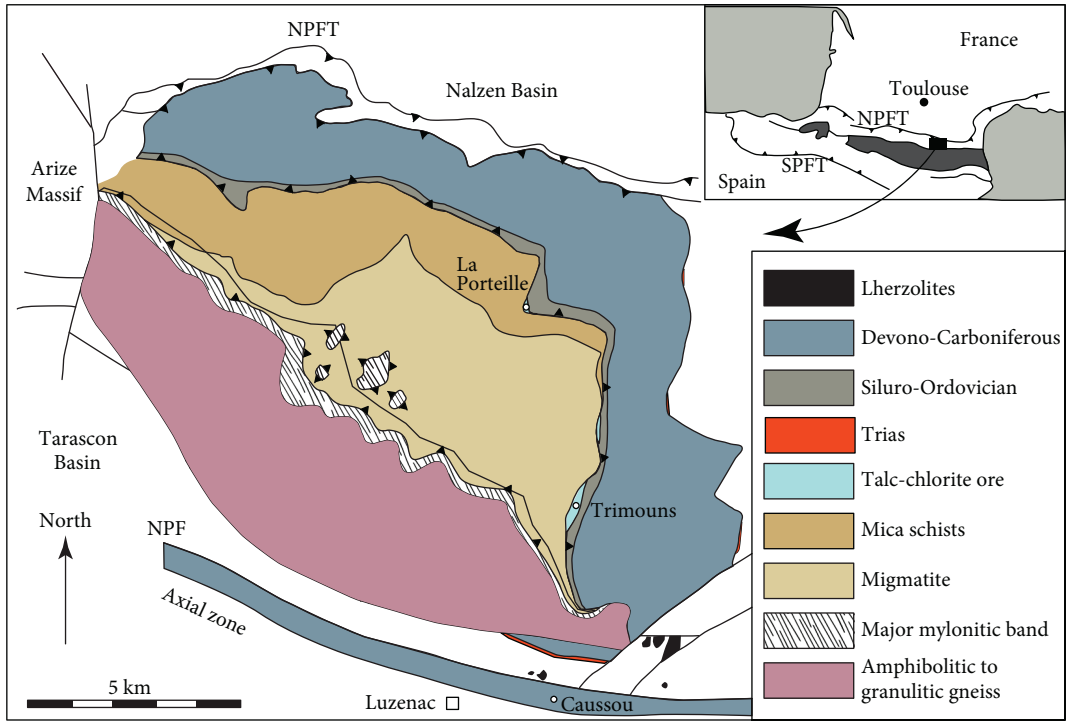

Figure 1: Simplified geological map of the Saint Barthelemy Massif (modified after [10, 32]).

1. Introduction

The circulation of fluids is known to play a crucial role both in the deformation of rocks and the transfer of heat and elements throughout the lithosphere. In the Pyrenees, there is a lot of evidence of widespread metasomatism attesting to large-scale fluid circulation in the crust. Three main types of metasomatism are recognized: (i) the albitization of the plutonic basement [1], (ii) the serpentinization of peridotite bodies ([2, 3]; Saint Blanquat et al., 2016), and (iii) the magnesian metasomatism expressed by the dolomitization, talcification, and chloritization of the basement ([4–8]; Core et al., 2017; [9]). All of these fluid/rock interaction systems were active between at least 122 Ma and 96 Ma [2, 10–14] and reached a climax during the Albo-Cenomanian regional hyperextension of the Pyrenean passive margin which led to mantle exhumation [15] and the high-temperature-low-pressure (HT/LP) metamorphism of the North Pyrenean Zone (NPZ) [11, 16–19]. This synchronism suggests strong links between fluid circulation, deformation, and heat transfers at the crustal scale in the Pyrenees as already proposed by some authors [11].

Beyond the effects of fluids on the thermomechanical behavior of the crust, the nature and origin of the different fluids that have circulated during the Albo-Cenomanian hyperextension remain poorly known. The occurrences of serpentinites, ophicalcites, albitites, talcitites, and chloritites all reflect the location of the main fluid pathways that were active during the Albo-Cenomanian period. Consequently, these evidences of metasomatism are excellent geological targets to characterize the fluid circulation systems active during this period.

This study is focused on the Trimouns talc-chlorite deposit (Figure 1) which represents the most prominent occurrence of Albo-Cenomanian magnesian metasomatism in the Pyrenees and one of the biggest talc deposits worldwide. Roughly 400000 tons of talc are produced annually, and close to around 20 million tons have already been extracted from this deposit. The current resources are estimated to be approximately 20 million tons [20]. Therefore, the large amount of fluid needed to form this talc deposit suggests that the Trimouns deposit represents one of the major drains at the scale of the Pyrenees.

In this paper, we characterize the fluid circulation system at the origin of the magnesian metasomatic system expressed at Trimouns by the widespread formation of dolostone, talc, and chlorite. Stable isotope analyses ($\delta^{13}C$, $\delta^{18}O$, δD, and $\delta^{37}Cl$), the Cl/Br ratio, and chlorinity measurements taken on fluid inclusions (FI) and their host minerals were used to document the paleofluid features and their possible origin. The objective is to relate the fluid geochemical signatures to the major fluid reservoirs and to constrain the potential migration pathways at the crustal scale that favored subsequent fluid-rock interaction at the origin of the deposit.

2. Geological Setting

The Pyrenees fold and thrust belt (Figure 1) result from two successive orogenies, the Variscan orogeny at the end of the Paleozoic, characterized by a polyphase compression history, and the Mesozoic-Cenozoic Alpine orogeny. The latter results from the inversion of a transcurrent hyperextended rift linked to the opening of the Bay of Biscay during the Cretaceous period [21–24]. This extreme

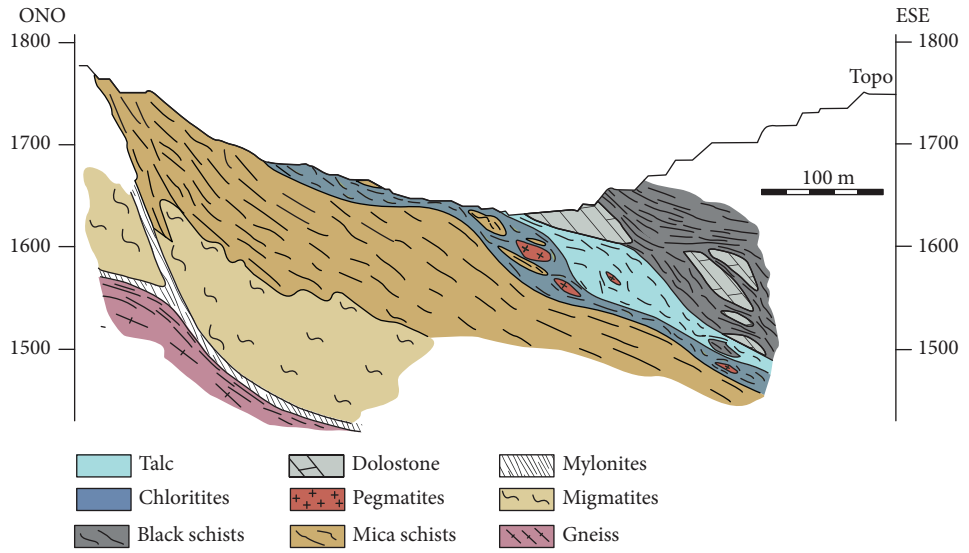

Figure 2: Synthetic cross-section through the Trimouns talc-chlorite deposit (from [7]).

thinning of the continental crust led to the local exhumation of the subcontinental mantle at the base of the Albo-Cenomanian basins [19, 25], occurring today as relicts of serpentinized peridotites in the North Pyrenean Zone [15]. The Albo-Cenomanian basins were formed during the opening of the Bay of Biscay which induced transtensive sinistral movements in the NPZ [22]. The basin formation was associated with a HT-LP metamorphism between *ca.* 113 and 85 Ma [16–18, 26–28]. To date, the consensus is to attribute this thermal anomaly to very high geothermal gradients related to the intense crustal and lithospheric thinning [11, 16–19].

In the NPZ, the circulation of large amounts of fluid under hydrothermal conditions is evidenced by the presence of numerous occurrences of talc-chlorite [6–8, 10], albitite [1, 12, 13], and serpentinized peridotite ([2]; Saint Blanquat et al., 2016). The Na-Ca metasomatism (albitization) is well dated between 110 and 92 Ma [12, 13] whereas the Mg metasomatism depicts widespread ages throughout the Pyrenees. The main talc formation episode is Cretaceous in age, dated between 122 and 96 Ma [10, 14] based on the U-Pb dating of REE-bearing minerals, particularly allanite formed in dolostone geodes [29, 30]. Lastly, the serpentinization event is supposed to be Albo-Cenomanian in age, even if it has still not been clearly dated yet, given the consistency of this age with the hyperthinning model for the crust and associated mantle exhumation [2].

The Trimouns deposit is localized at the eastern edge of the Saint Barthelemy Massif (SBM) (Figure 1). From the base to the top, the SBM is composed of (i) amphibolitic to granulitic gneiss, (ii) migmatites and mica schists, and (iii) middle to upper Paleozoic series including Ordovician to Devonian schists, quartzite, and Silurian black schists and marbles [31–33]. Dolostones occur in the Paleozoic succession, but their origin remains a matter of debate. Some authors suggest that they are Ordovician [31] whereas others suggest that they were formed during Albo-Cenomanian times, via the metasomatism of the Silurian marbles [6]. The contact between the mica schists and carbonate rocks and the Silurian black schists is tectonic and corresponds to a fault considered to be a decollement level located within the Silurian black schists [10]. Talc and chlorite occur as lenses that are discontinuously distributed along this tectonic interface where mineralizing fluid(s) has/have been channelized. In further detail (Figure 2), chlorite ore is localized above the footwall of the fault where mica schists and, locally, pegmatites occur. Talc ore is mainly localized at the hanging wall of the fault composed of dolostones, marbles, and schists, from the Siluro-Devonian series (Figure 1). This spatial distribution of the two ores results from different interlinked chemical reactions driven by the nature of the metasomatized parent rock.

3. Constraints on the Fluid Circulation System

3.1. The Metasomatic Alteration. At Trimouns, talc can be formed following two main reactions:

(1) The interaction between the dolostones and a silica-rich fluid [8]

$$3CaMg(CO_3)_2 + 4SiO_{2(aq)} + 6H^+ = Mg_3Si_4O_{10}(OH)_2 + 3Ca^{2+} + 6CO_2 + 6H_2O \quad (1)$$

(2) A direct fluid oversaturation with respect to the talc, e.g., a fluid enriched in Mg and Si [8]

$$4SiO_{2(aq)} + 3Mg^{2+} + 4H_2O = Mg_3Si_4O_{10}(OH)_2 + 6H^+ \quad (2)$$

The Mg(Fe) chlorite formation is dependent from both Mg supply and Al availability, which is known to be poorly

mobile. This explains why chlorite ore (mainly clinochlore, [29]) forms mostly at the expense of mica schists and pegmatites, which are rich in aluminous minerals (mainly muscovite and plagioclase) and quartz. According to Moine et al. [8], the aluminum needed to form chlorite primarily comes from the dissolution of muscovite in mica schists following the reaction:

$$2KAl_2Si_3AlO_{10}(OH)_2 + 3SiO_2 + 15Mg^{2+} + 24H_2O = 3Mg_5AlSi_3AlO_{10}(OH)_8 + 2K^+ + 28H^+ \quad (3)$$

whereas in pegmatites, the main source of aluminum is plagioclase [29]. The formation of chlorite from plagioclase can be expressed as follows:

$$2NaAlSi_3O_8 + 5Mg^{2+} + 8H_2O = Mg_5AlSi_3AlO_{10}(OH)_8 + 2Na^+ + 6H^+ + 3SiO_2 \quad (4)$$

$$\text{or } CaAl_2Si_2O_8 + SiO_2 + 5Mg^{2+} + 8H_2O = Mg_5AlSi_3AlO_{10}(OH)_8 + Ca^{2+} + 8H^+ \quad (5)$$

As shown above, a silica supply is needed to form both chlorite and talc. Fortuné (1980) and De Parseval [29] suggested that silica was leached from quartz present in the hosting rocks of the deposit (pegmatites and mica schists). The dissolution of most silicates, except tourmaline, and their replacement by talc confirm that silicates are all unstable in the presence of mineralizing fluids. The excess silica precipitated around the talc body as discrete euhedral quartz in the dolostone geodes, together with euhedral calcite, dolomite, and talc (Figure 3).

Ca^{2+} and CO_2 leached out during talc formation from dolostones induce the formation of calcite ([7, 29], the so-called hydrothermal calcite from [6]), which occurs in geodes or crosscutting dolostones as veins (Figure 3). Based on the similar REE compositions, $\delta^{18}O$ and $\delta^{13}C$ values, and $^{87}Sr/^{86}Sr$ ratios, Boulvais et al. [6] showed that hydrothermal calcite formed from a single fluid event under a variable fluid-rock ratio.

Based on reactions (2), (3), (4), and (5), an additional supply of magnesium is needed to precipitate the talc and to form the chlorite via the alteration of the pegmatites and mica schists. The source of magnesium is still a matter of debate: either the magnesium is provided by the fluid itself (Fortuné, 1980; [10, 29]) or it is acquired by the mineralizing fluid interacting with encountered percolated rock from the source to the deposit.

3.2. The Mineralizing Fluid. Several studies have attempted to characterize the nature of the mineralizing fluid(s) and its physical circulation conditions. Based on a microthermometric study of the fluid inclusions hosted by the euhedral quartz localized in pods and inferred to be synchronous with Mg metasomatism, Moine et al. [8] proposed that the main mineralizing fluid was a brine (~25 wt% eq. NaCl) that circulated at about 300°C and 1.5 kbar. De Parseval et al. [31] came to the same conclusions based on a study of the fluid inclusions hosted by (i) the quartz pods in chloritite ore, (ii) the fluorapatite in the chloritite ore, and (iii) the allanite observed in the dolostone geodes (as shown in Figure 3). In these two studies, the P-T conditions rely solely on the consideration of fluid inclusion isochors and no independent pressure or temperature estimates are available which means that the P-T path is a hypothetical estimation. The main mineralizing fluids were evaporated seawater saturated with respect to halite on the basis of the chlorinities and the Cl/Br ratio (values from 140 to 565) that circulated between 250-280°C and 0.4 to 2 kbar [4, 5, 34]. These brines contain traces of N_2-$CO_2 \pm CH_4$ and a low magnesium content [5].

All of these studies conclude that primary brines are probably responsible for the talc ore formation. These brines are supposed to be synchronous with the deposition of the nearby Triassic evaporites. A stable isotope study ($\delta^{13}C$, $\delta^{18}O$, and δD) of the whole metasomatic sequence, from unaltered marbles to dolostones to hydrothermal minerals (talc, chlorite, calcite, and quartz), suggested that both the dolomitization and talc-chlorite ore formation stages resulted from the same continuous hydrothermal event [6]. This implies that the supply of an allochthonous magnesium source was transported by the mineralizing fluid. Even though the authors suggest that the main fluid reservoir was Albian seawater, an (minor) involvement of secondary brines is also suggested. Lastly, Boutin [7] provided an extended thermometric study of the different chlorites occurring at Trimouns in order to discuss the range of temperatures for the formation of the deposit. He concluded that the chlorite in the deposit formed between 275°C and 350°C with a first mode at around 275°C and a second one at around 325°C.

To summarize, from previous studies, it appears that the main fluid(s) at the origin of the talc-chlorite ore deposit probably was/were brine(s) that circulated at a temperature of 300 ± 50°C [4, 5, 7, 8, 31, 34]. However, the origin(s) of the brine(s) has/have not been clearly addressed. It has also been suggested that the whole metasomatic sequence, from dolomitization to hydrothermal mineral formation (talc, chlorite, calcite, and quartz), resulted from the same continuous hydrothermal event [6].

The main objectives of this work are to characterize the type of brines (primary vs. secondary) involved in the formation of the talc-chlorite deposit and to determine if these brines have been mixed with other types of fluids. The spatial extent of the fluid circulation system is specified by analyzing the regional sample. Following the hypothesis of Boulvais et al. [6], the fluids at the origin of dolomitization and talc-chlorite formation are compared in order to determine if the whole metasomatic sequence resulted from the same hydrothermal event. Lastly, the possible sources of fluids involved in the magnesian metasomatic system recorded at Trimouns are discussed in order to constrain their potential migration pathways at the crustal scale.

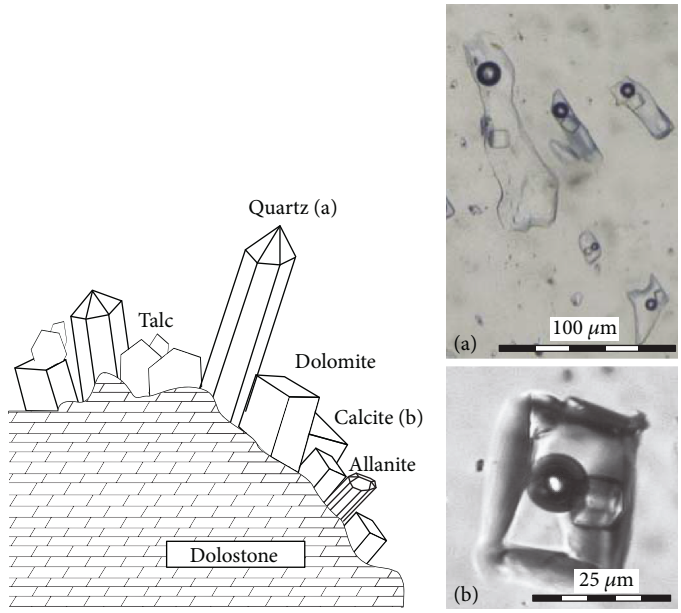

Figure 3: Schematic sketch illustrating the various studied minerals observed in the geodes, from where the samples were taken. (a) Typical fluid inclusions hosted by euhedral quartz; (b) typical fluid inclusions hosted by hydrothermal calcite.

4. Methods

4.1. Sampling Strategy. Several minerals considered to have been synchronous with the main talc formation stage were sampled: (i) euhedral quartz and hydrothermal calcite, both occurring in geodes hosted by dolostones and (ii) calcite veins crosscutting dolostones (Figure 3). Euhedral quartz and calcite are considered synchronous with the main talc formation since, in geodes, they are spatially and texturally associated with euhedral talc and with REE minerals (mainly allanite). The calcite veins crosscutting the dolostones are either (i) thin fractures (≤2 cm) filled by massive calcite or (ii) thicker veins (≥10 cm) filled by euhedral calcite and considered to be tension gashes. As explained previously, these calcite occurrences are supposed to be by-products of the transformation of dolostone into talc [6, 7, 29] and are consequently considered as hydrothermal calcite [6]. In the following sections, the term "hydrothermal calcite" will refer to the thin and thick calcite veins crosscutting the dolostone sampled for this study. In order to demonstrate the genetic link between the dolomitization stage and the talc-chlorite ore formation stage suggested by Boulvais et al. [6], a series of dolostones was sampled. These samples are massive and undeformed dolostones localized in the hanging wall of the deposit. The intergranular porosity is filled by talc, chlorite, and organic matter. As described above, these dolostones host geodes and calcite veins.

Lastly, the quartz-calcite veins occurring in the Devonian schist located at the southern part of the deposit (Caussou, Figure 1) were sampled in order to characterize the possible spatial extension of the mineralizing fluid circulation. They represent further evidence of fluid circulation in the close vicinity of the deposit; however, no geochronological constraints are available. This sample comes from a geometrically complex network of quartz-calcite veins localized along a main fault in a deformation zone affecting the Devonian schist (Figure 4). This network attests to the circulation of a significant amount of fluid in this deformation zone located just to the south of the North Pyrenean Fault.

4.2. Fluid Inclusions

4.2.1. Salinity Measurements and Absolute Cl Content. Fluid inclusions were studied by microthermometry using a Linkam heating-freezing stage. The fluid inclusions used for the calibration were a pure CO_2 natural standard fluid inclusion from Camperio (triple point at -56.6°C) and H_2O-NaOH synthetic fluid inclusions (ice melting temperature at -0.4°C). The accuracy at high temperature is ±2°C. The salinities were determined via either the f ice melting temperature or the melting temperature of the salt cubes when present.

In dolostones, fluid inclusions are very small and the microthermometric measurements for Tm ice are rather difficult to obtain. Thus, the salinity was obtained by Raman spectroscopy at room temperature using the methodology published by Dubessy et al. [35] and Caumon et al. [36]. The typical model uncertainty is ±0.3 mass% NaCl (after the revision of the calibration curve in [36]).

The average Cl content of the fluid inclusions for the various samples was estimated based on the average salinity value calculated from the whole salinity dataset for each type of fluid inclusion.

4.2.2. Cl/Br Ratio. The bulk Cl and Br contents of the water trapped in the fluid inclusions were determined at the Université de Lorraine, GeoRessources, Vandoeuvre-lès-Nancy, France, using the bulk crush-leach technique described by Banks and Yardley [37], Banks et al. [38], and Gleeson et al. [39]. The quartz and carbonate veins were crushed to a grain size fraction of at least 1–2 mm. The pure mineral separates were then picked and placed in an ultrasonic bath for a

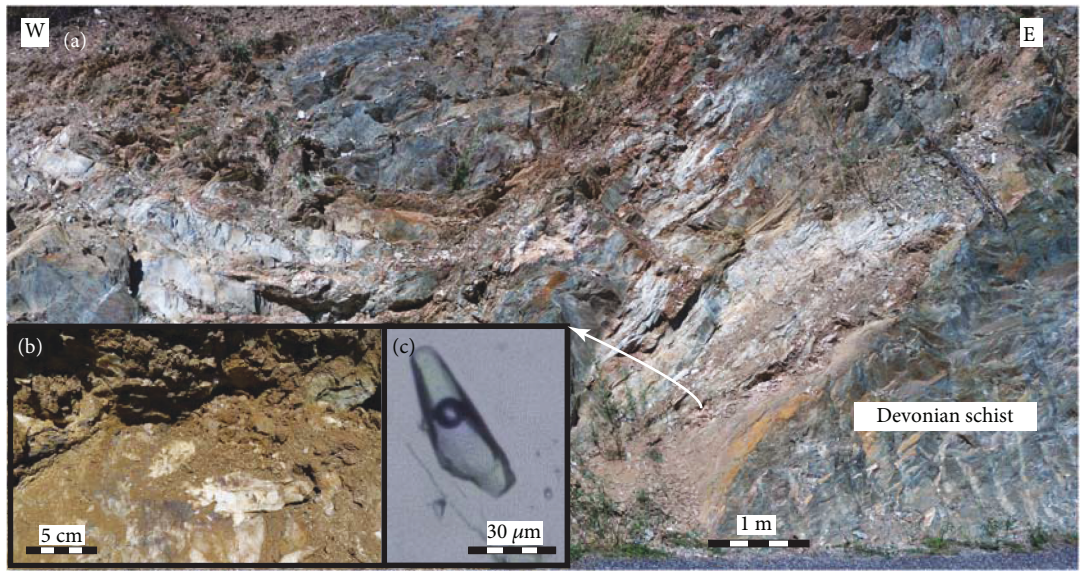

Figure 4: (a) Field view of the Caussou sampling site with (b) a zoom on a quartz-calcite vein and (c) a typical fluid inclusion hosted in quartz.

maximum of 1 hour. Then, the samples were cleaned by boiling twice in Milli-Q water. The cleaned quartz and carbonate grains were then crushed to a fine powder in an agate pestle and mortar and leached by Milli-Q water.

Leachates from the fluid inclusions were analyzed for Cl and Br with a Dionex DX-500 ion chromatograph. The detection limit for the anions in the fluid inclusion leachates was 3 ppb for Cl and 1 ppb for Br. The results are expressed as a Cl/Br molar ratio.

4.2.3. $\delta^{37}Cl$. Stable isotope analyses were performed on the same bulk leachate as those used to measure the Cl/Br molar ratio as explained in the previous section. The sample preparation technique for the $\delta^{37}Cl$ analysis using CH_3Cl as a working gas has been described in detail elsewhere [40–43]. It consists of (1) the precipitation of chloride as AgCl, (2) the methylation of AgCl to gaseous CH_3Cl, and (3) the purification of CH_3Cl via separation from the excess CH_3I in the two GC columns filled with Porapak Q. The $\delta^{37}Cl$ values are then determined on purified CH_3Cl gas with a DI-IRMS (Thermo Finnigan, Delta plus XP) at the Laboratoire de Géochimie des Isotopes Stables (Institut de Physique du Globe de Paris and Université Paris 7). $\delta^{37}Cl$ is expressed as the permil deviation relative to the standard SMOC (Standard Mean Ocean Chloride). Every seventh sample, a series of three seawater standard isotopic compositions was measured in order to estimate the reproducibility of the analyses. For each session (10 measurements), the $\delta^{37}Cl$ values of the samples were corrected by the mean seawater isotopic composition of the session. For this study, at least two measurements were taken from the same leachates during the various analytical sessions. Lastly, the isotopic compositions of the samples are the mean value of the duplicate. The uncertainty associated with each sample corresponds to the standard deviation and is lower than 0.1‰. During the course of this study, the external reproducibility on the seawater standard was 0.00 ± 0.04‰ (1σ, $n = 18$), as routinely obtained at IPGP for over two decades now [40, 44, 45].

4.2.4. δD. Fluids trapped in the quartz, hydrothermal calcite, and dolostones were extracted by crushing under vacuum. Grains weighing from 1.0 to 6.7 g and measuring several millimeters to centimeter were loaded into steel tubes and degassed overnight at 120°C under vacuum in order to release any water adsorbed at the mineral surface. H_2O was separated cryogenically from other gases and reduced into H_2 through a uranium reactor at 800°C. The D/H ratios of the H_2 gases were measured using a GV IsoPrime mass spectrometer at CRPG (Vandoeuvre-lès-Nancy, France). The results are expressed in δ notation in permil relative to the V-SMOW-SLAP scale. Two CRPG internal water standards were analyzed along with each weekly batch of water samples obtained from the fluid inclusions. To detect any potential effect of memory on the D/H ratios within the uranium reactor, the samples were duplicated whenever possible. This effect was not detected, but slight variations in δD for some samples were recorded. Given that these variations probably reflect variations in the δD composition within the fluid inclusion population, all of our duplicate measurements are presented here. They are denoted by adding the letter a, b, or c to the sample name in Table 1. The reproducibility for the standards was estimated to be lower than 2‰.

4.3. Host Minerals

4.3.1. $\delta^{18}O$ and $\delta^{13}C$ in Dolostones and Hydrothermal Calcite. Isotopic measurements were taken at the CRPG laboratory (Vandoeuvre-lès-Nancy, France). The carbon and oxygen isotopic compositions of the dolostones and hydrothermal calcite were measured using a GasBench autosampler coupled to a Thermo Scientific MAT253 isotope ratio mass spectrometer (IRMS). The residual dolostone and hydrothermal calcite powders were collected after crushing in order to obtain the δD measurements for the fluid inclusions. An aliquot between 200 and 400 μg of fine powder was reacted

Table 1: The Cl/Br and deuterium, chlorine, and recalculated oxygen isotopic compositions of the fluid inclusion water hosted by the different samples and the oxygen and carbon isotopic composition of the host minerals.

Sample	Description	Localization	δD vs. SMOW	δ^{18}O vs. SMOW	δ^{13}C vs. PDB	δ^{18}O fluid (300°C)	δ^{37}Cl vs. SMOC	Cl/Br
Qz-Geo-1a	Euhedral quartz in geode in dolostone	Trimouns	-26.0	11.8		5.8		
Qz-Geo-1b	Euhedral quartz in geode in dolostone	Trimouns	-32.6	11.7		5.7		
Qz-Geo-2a	Euhedral quartz in geode in dolostone	Trimouns	-46.7	10.4		4.4		
Qz-Geo-2b	Euhedral quartz in geode in dolostone	Trimouns	-49.7	11.3		5.3	-0.58	428
Qz-Geo-2c	Euhedral quartz in geode in dolostone	Trimouns	-43.9	x		x		
Qz-Geo-3a	Euhedral quartz in geode in dolostone	Trimouns	-33.1	11.2		5.2	-0.55	515
Qz-Geo-3b	Euhedral quartz in geode in dolostone	Trimouns	-38.5	11.0		5.0		
Qz-Geo-4a	Euhedral quartz in geode in dolostone	Trimouns	-36.0	11.1		5.1	-0.41	540
Qz-Geo-4b	Euhedral quartz in geode in dolostone	Trimouns	-48.1	11.0		5.0		
Qz-Geo-5a	Euhedral quartz in geode in dolostone	Trimouns	-29.0	12.2		6.2		
Qz-Geo-5b	Euhedral quartz in geode in dolostone	Trimouns	-25.6	11.3		5.3		
Qz-Geo-6	Euhedral quartz in geode in dolostone	Trimouns	-28.5	12.2		6.2		
Qz-Geo-7	Euhedral quartz in geode in dolostone	Trimouns					0.14	395
Qz-Geo-8	Euhedral quartz in geode in dolostone	Trimouns					-0.34	609
Cal-1	Hydrothermal calcite	Trimouns	-44.1	8.8	-3.2	3.0	-0.22	390
Cal-2a	Hydrothermal calcite	Trimouns	-66.2	9.1	-2.3	3.3	0.14	405
Cal-2b	Hydrothermal calcite	Trimouns	-65.4	9.0	-2.2	3.3		
Cal-3	Hydrothermal calcite	La Porteille	-64.6	9.0	-2.7	3.2	0.87	319
Qz-Caus-1	Quartz from Qtz-Cal vein in Devonian schist	Caussou	-45.0	23.5		17.5	-0.12	571
Cal-Caus-1a	Calcite from Qtz-Cal vein in Devonian schist	Caussou	-38.3	20.7	-0.8	14.9		682
Cal-Caus-1b	Calcite from Qtz-Cal vein in Devonian schist	Caussou	-36.5					
Dol-1a	Dolostone	Trimouns	-23.4	9.9	-0.6	3.9	-0.43	360
Dol-1b	Dolostone	Trimouns	-27.2	9.5	-0.8	3.5		
Dol-2	Dolostone	Trimouns	-37.3	10.0	-0.7	4.0	-0.09	269
Dol-3a	Dolostone	Trimouns	-33.7			x	-0.13	307
Dol-3b	Dolostone	Trimouns	-32.8	10.0	-0.3	4.0		
Dol-4	Dolostone	Trimouns	-27.6	9.8	-0.4	3.8	-0.22	299

with 2 mL of supersaturated orthophosphoric acid at 70°C for at least 10 hours in a He atmosphere. Ten measurement cycles of the produced CO_2 isotopic composition were performed with the Thermo Scientific MAT 253 continuous flow isotope ratio mass spectrometer. The isotopic compositions are given in the delta notation in ‰ relative to V-PDB for carbon and converted to V-SMOW for oxygen. The sample measurements were adjusted to the internal reference material (Merck synthetic calcite) calibrated using international standards IAEA CO-1, IAEA CO-8, and NBS 19.

In order to remain consistent with the D/H measurements, the samples were duplicated and the values are presented (denoted as "a," "b," or "c"). The reproducibility for the standard was less than 0.05‰ for $\delta^{13}C$ and 0.1‰ for $\delta^{18}O$.

4.3.2. $\delta^{18}O$ of Quartz. The $\delta^{18}O$ isotopic analysis of the quartz samples was performed at the Laboratoire de Géochimie des Isotopes Stables (Institut de Physique du Globe de Paris and Université Paris 7). The isotopic compositions are given in the standard delta notation in ‰ relative to V-SMOW for oxygen. The samples were finely crushed and reacted with BrF_5 as an oxidizing agent overnight in Ni tubes at 550°C following the method described by Clayton and Mayeda [46]. The O_2 was directly analyzed on a Thermo Fisher DELTA V mass spectrometer. During the course of the analyses, the NBS28 quartz standard measurements were used to confirm the general reliability of the protocol (mean $\delta^{18}O = 9.67 \pm 0.2‰$, $n = 4$). In order to stay consistent with the δD measurements, the samples were duplicated and both values are presented (denoted as "a" or "b"). Each sample corresponds to the residual quartz powder after crushing.

5. Results

5.1. Description and Salinity of the Fluid Inclusions. Fluid inclusions (FI) from the euhedral quartz and hydrothermal calcite display similar features (Figure 3): they are aqueous, most of them are saturated at an ambient temperature with respect to halite (i.e., they contain a halite cube), and their liquid/vapor ratio ranges between 10% and 30%. The salinity measurements display a narrow and similar range for both the euhedral quartz and hydrothermal calcite with an average salinity of 28.6 wt% eq. NaCl and 30.5 wt% eq. NaCl, respectively (Figure 5 and Table 2). The homogenization temperature (Th) of the fluid inclusion in the quartz and calcite ranges from 130° to 230°C. Traces of gases, in particular N_2 (>60 mol% in the volatile phase and minor amounts of CO_2 and CH_4), were found by Raman spectroscopy.

There are numerous but small fluid inclusions in dolostones (1 μm < FI diameter < 5 μm) making it difficult to carry out petrographic and microthermometric studies. The studied fluid inclusions are aqueous (L-V inclusions), with a high salinity ranging between 20.8 and 29.6 wt% eq. NaCl with a mean value at 25.0 wt% eq. NaCl (Figure 5 and Table 2). Due to the small size of the fluid inclusions in the dolostones, it has been impossible to determine the traces of gas.

For the regional samples (Caussou 1), the aqueous fluid inclusions in the quartz do not have halite cube (Figure 4(b)). The mean salinity value is at 25.6 wt% eq. NaCl (Table 2). The Th values range between 190 and 200°C. Gases are only present as traces of predominant CO_2 (>95 mol% in the volatile phase and several mol% of N_2).

For the different minerals, it appears that the features of the fluid inclusions are similar with high salinity, a homogenization temperature close to 200°C, and, when it has been measured, traces of gas.

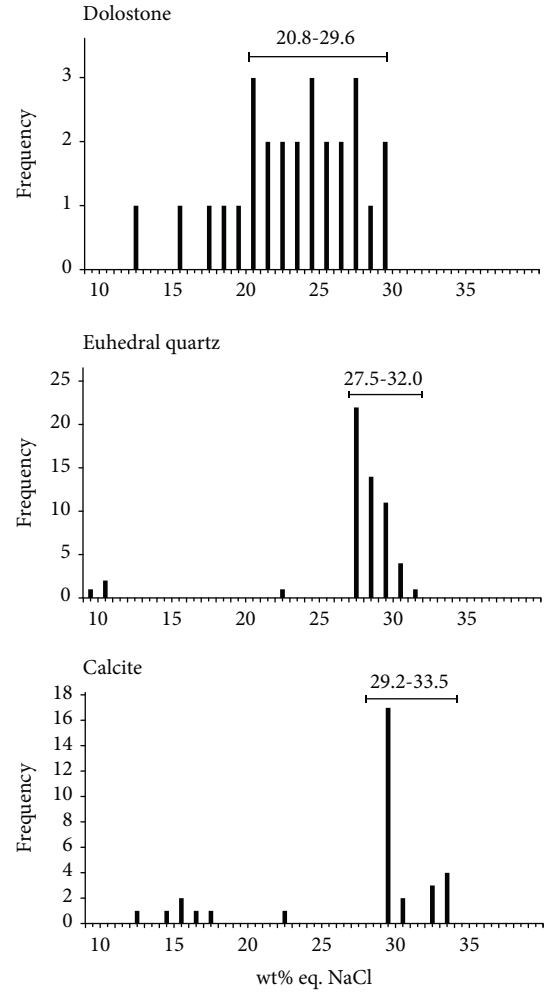

Figure 5: Histogram of the salinities (wt% eq. NaCl) from the microthermometric and Raman analyses for the different samples.

5.2. Cl/Br, $\delta^{37}Cl$, and δD of the Fluid Inclusions and $\delta^{18}O$ and $\delta^{13}C$ of the Host Minerals. All of the results are presented in Table 1. The fluid inclusions hosted in the euhedral quartz, hydrothermal calcite, and dolostone display very similar isotopic and Cl/Br ratios. Figure 6 shows the Cl/Br ratios as a function of the chlorinity. Based only on the Cl/Br ratio, all of the samples fall in the field of evaporated seawater saturated with respect to halite. The fluid inclusions hosted in the dolostones and hydrothermal calcites have similar Cl/Br ratios centered at around 350 whereas the fluid inclusions hosted in the quartz have a higher Cl/Br ratio of up to 609. The fluid from the Caussou calcite sample is the only one to fall above the Cl/Br value of seawater reaching 682 (Table 1). Based on Figure 6, no correlation is identified between the Cl/Br and chlorinity variations in the fluid inclusions hosted in the different samples.

For the $\delta^{37}Cl$ values, most of the samples fall in the field of evaporated seawater between 0‰ and -1‰ (Figure 7). The fluids from one quartz and two hydrothermal calcites shifted to positive $\delta^{37}Cl$ values with only one sample significantly shifting up to 0.87‰ (Table 1). This sample is a hydrothermal calcite sampled in the La Porteille area, the northern extension of the deposit (Figure 1). As represented in

Table 2: Fluid inclusion salinities of the studied samples.

Type of sample	n	Mode wt% eq. NaCl	Av. salinity wt% eq. NaCl	σ	Av. Cl (ppm)	σ
Trimouns/La Porteille						
Hydrothermal calcite	26	29.2-33.5	30.5	1.5	186050	9150
Dolostone	21	20.8-29.6	25.0	2.7	152500	16470
Euhedral quartz	52	27.5-32	28.6	1	174460	6100
Caussou						
Quartz	9	24.5-26.2	25.6	0.6	156160	3660

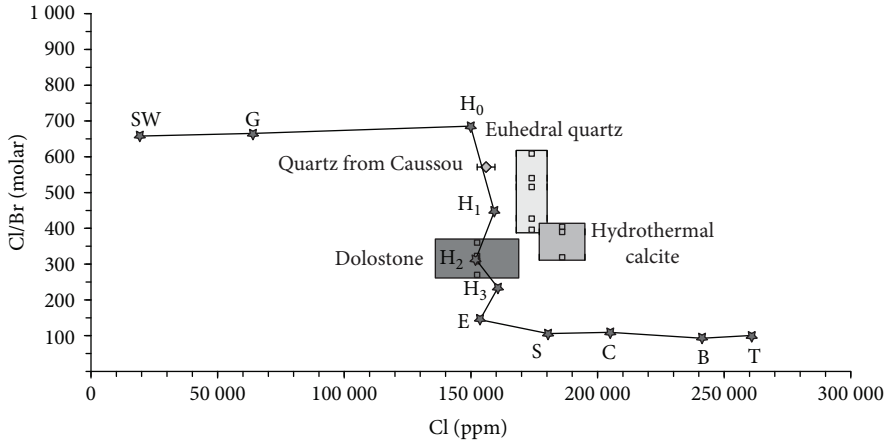

Figure 6: Cl/Br vs. Cl graph of the compositions of the water contained in the different samples. The horizontal extents correspond to the standard deviation of the chlorinity (Table 2) and the vertical extents of the maximum and minimum values of the Cl/Br ratio for the samples (Table 1). Seawater evaporation trend taken from Fontes and Matray [51]. SW: seawater; G: gypsum; H: halite (H_0: beginning of halite precipitation → H_3: end of the halite precipitation); E: epsomite; S: sylvite; C: carnallite; B: bischofite; T: tachyhydrite.

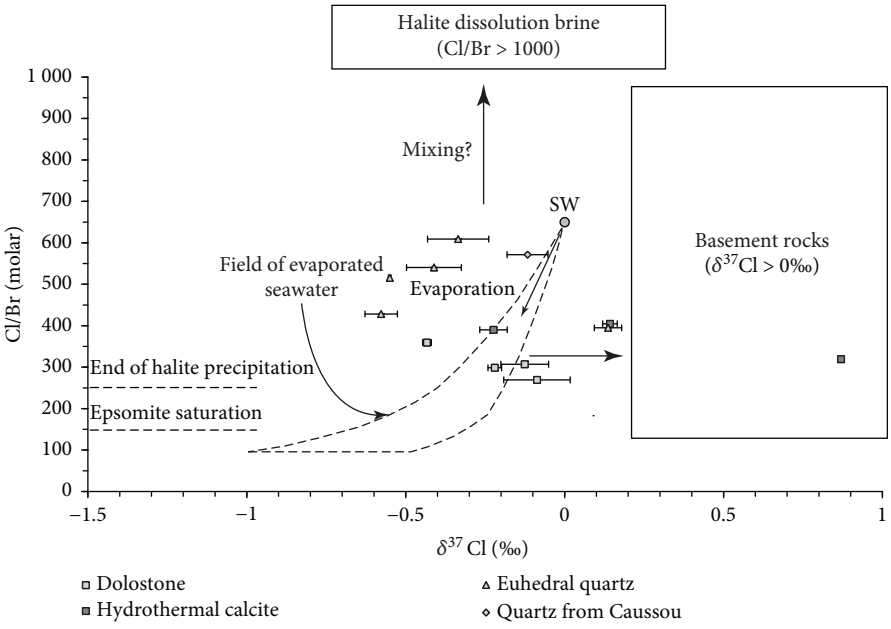

Figure 7: δ^{37}Cl vs. Cl/Br diagram where the composition of the brines hosted by the different samples is represented (adapted from [53]). Evaporated seawater field following Fontes and Matray [51], Eggenkamp et al. [50], and Eastoe et al. [49]. SW: seawater.

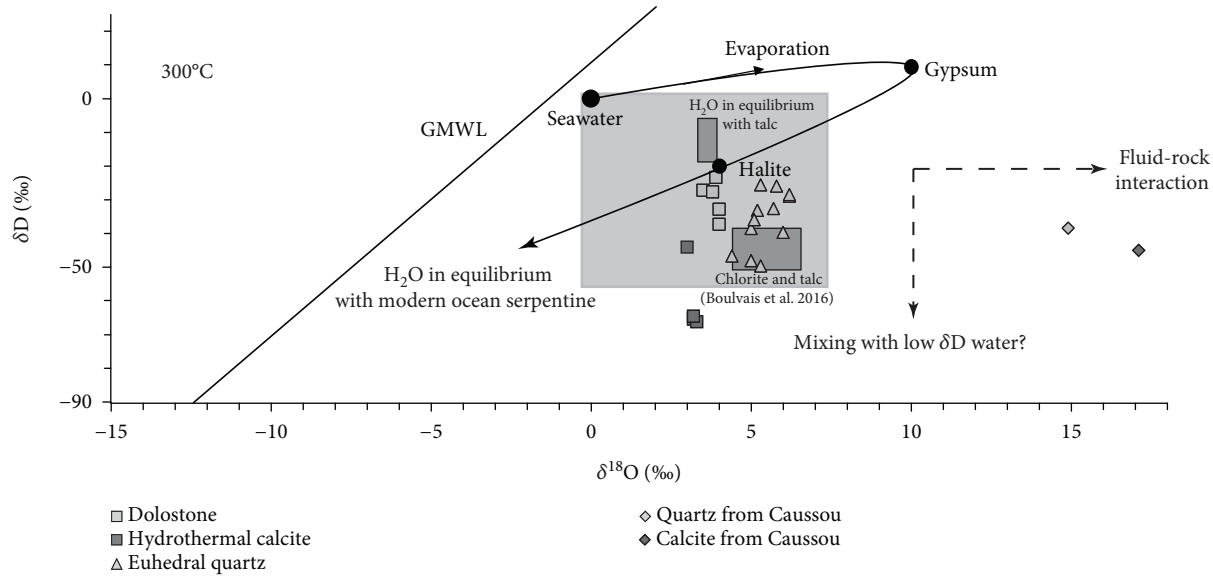

Figure 8: δD vs. δ^{18}O for the water hosted by the different samples (adapted from [58]). The δ^{18}O values for the fluid inclusion water were calculated assuming that the host mineral precipitation occurred at 300°C using the fractionation coefficient given by Zheng [47, 48]. Seawater evaporation trend taken from Holser [56] and Knauth and Beeunas [57]. GMWL: Global Meteoric Water Line.

Figure 7, when combined with the Cl/Br ratio, numerous samples plot out of the evaporated seawater field. This could suggest the mixing of evaporated seawater saturated with respect to halite with seawater and/or with brine formed by the dissolution of halite (secondary brine).

For the δD and δ^{18}O values, most of the samples (except two from Caussou) have similar δ^{18}O values ranging between 9‰ and 12.2‰ whereas the δD values are more variable and range between -25.6‰ and -66.6‰. Variations in the δD and δ^{18}O values are correlated to the mineral in which the fluid inclusions are hosted. The euhedral quartz has higher δ^{18}O values, the dolostones have intermediate values, and the hydrothermal calcites have the lowest δ^{18}O values. For the δD values, the euhedral quartz and dolostone have similar values whereas the hydrothermal calcites display the lowest ones (around -65‰). These relationships are well illustrated in Figure 8 which displays the δD values directly measured in the fluid inclusions and the δ^{18}O values of the fluid recalculated using the oxygen isotopic composition of the hosted minerals and the adapted isotopic fractionation coefficients [47, 48] at 300°C. As mentioned previously, only the quartz and calcite samples from Caussou have significantly shifted from the main field with δ^{18}O values of 23.5‰ and 20.7‰, respectively, and δD values of -45‰ for the quartz and between -36.5‰ and -38.3‰ for the calcite.

For δ^{13}C values, both hydrothermal calcite and dolostone have similar values (between -3.2‰ and -2.2‰ and between -0.8‰ and -0.3‰, respectively) than those presented and discussed by Boulvais et al. [6]. Calcite from Caussou has a carbon isotopic composition of -0.8‰.

6. Discussion

The first part of this section deals with the characterization of the nature of the mineralizing fluid(s) at the origin of the magnesian metasomatism expressed at Trimouns through widespread dolomitization and talc-chlorite formation. Although previous studies have argued that the main fluid(s) at the origin of the talc-chlorite ore deposit was/were probably brine(s) that circulated at a temperature of 300 ± 50°C [4, 5, 7, 8, 31, 34], the nature of the brine(s) (primary vs. secondary) and the possible involvement of other types of fluid(s) have not been clearly addressed. The interaction of the mineralizing brine(s) with the hosting rock of the deposits is also discussed in order to determine if the dolomitization and talc-chlorite formation result from a single fluid circulation event as previously suggested by Boulvais et al. [6]. Finally, the signification of the fluid event documented in Caussou (Figure 1) is discussed in order to determine the potential spatial extent of the mineralizing brine circulation system at a multikilometer scale.

The second part of this discussion deals with the determination of the source of the mineralizing brine(s) based on the particular geological context of the area during the Albo-Cenomanian period. The goal of this work is to propose a fluid circulation model at the crustal scale that is focused on the Trimouns deposit.

6.1. Nature, Interaction, and Spatial Extent of the Mineralizing Brine(s) in the Trimouns Area

6.1.1. Primary Signature of the Mineralizing Brine(s)

(1) Chlorine Proxies (Salinity, Cl/Br, and δ^{37}Cl). The fluid inclusions hosted by the minerals that are synchronous with the talc primarily have high salinities between 27.5-32.0 wt% eq. NaCl and 29.2-33.5 wt% eq. NaCl for the euhedral quartz and hydrothermal calcite, respectively (Figure 5 and Table 2). However, few moderate salinities are also measured in the fluid inclusions (quartz: 10-15 wt% eq. NaCl; calcite: 12-

18 wt% eq. NaCl). There are two ranges for salinity in the dolostones: a major one corresponding to highly saline fluids at approximately 25 wt% eq. NaCl (20.8 and 29.6 wt% eq. NaCl, max at 29.6 wt% eq. NaCl) and a second minor one corresponding to a more diluted fluid at about 12-15 wt% eq. NaCl. The general high salinity of the fluids is consistent with the fact that the main mineralizing fluid has passed the halite saturation point. However, moderate salinities should reflect minor mixing with another more diluted fluid.

The δ^{37}Cl signature and the Cl/Br ratio of a fluid are powerful proxies to determine the nature of the brines [49–51]. Fontes and Matray [51] have demonstrated that during the evaporation of seawater, the Cl/Br ratio has a typical evolution correlated with the increasing chlorinity of the residual solution. Here, our data, gathered as boxes, plot close to the evaporation line (Figure 6). The box for the dolostones is consistent with the area of the primary brines saturated with respect to halite. For the hydrothermal calcite and euhedral quartz, the Cl/Br ratios are also consistent with those expected for a primary brine having passed the halite saturation point; however, the chlorinities are slightly to significantly higher (up to Cl ≈ 200000 ppm). Two main processes may increase the chlorinity. The first one is a reequilibration of the primary brines with halite at higher temperatures—the solubility of halite increases with temperature. In this case, the Cl content is increased but not the Br content and the data are shifted to higher Cl/Br ratios. The second process corresponds to an uptake of water. The replacement of anhydrous minerals (dolomite, feldspars, and plagioclases) by hydrated minerals (talc and chlorite) increases the chlorinity during the alteration of the crystalline basement by fluids. This process has already been suggested in unconformity U-type deposits hosted in the Athabasca Basin in Canada [52, 53], in the Modum Complex in Norway [39], and in the Schwarzwald district in Germany [54, 55].

If we consider the δ^{37}Cl values, all of the fluid inclusions hosted in the dolostones, euhedral quartz, and hydrothermal calcite have isotopic compositions (-0.58‰ to 0.14‰, Table 1) that are consistent with those expected for evaporated seawater ($-0.9‰ \leq \delta^{37}Cl \leq 0.2‰$, [49, 50]). Only one sample (PORT-2B, $\delta^{37}Cl = 0.87‰$) displays a significantly higher value, which may reflect the influence of a more intense fluid/basement interaction since biotite and amphibolite are known to be the main Cl-bearing minerals in igneous and metamorphic rocks and to have positive δ^{37}Cl values ([53] and references herein). With respect to the combination of the Cl/Br ratio and the chlorine isotopic compositions (Figure 7), the whole magnesian metasomatic sequence is either in or close to the field of evaporated seawater.

(2) Hydrogen and Oxygen Isotopic Systems. Figure 8 represents the hydrogen and oxygen isotopic composition of the water trapped in fluid inclusions hosted in the studied samples calculated at a temperature of 300°C. This figure also shows the position of (i) the seawater, (ii) the present-day Global Meteoric Water Line, (iii) the seawater evaporation trend [56–58], (iv) the isotopic composition of the talc and chlorite from Trimouns [6], and (v) the water in isotopic equilibrium with the talc (oxygen isotope data from [59]; hydrogen isotope data from [60]).

All of the waters from the dolostones, euhedral quartz, and hydrothermal calcite are broadly either in or close to the ideal range of isotopic compositions of the evaporated seawater saturated with respect to halite. The range of isotopic compositions of the water in equilibrium with the talc from Trimouns [6] also plots in this field. In more detail, all of our data are slightly depleted in deuterium and euhedral quartz and are also slightly shifted to more positive δ^{18}O values. This general trend toward more negative δD values can be explained by mixing evaporated seawater with a low δD fluid. The possible source of this type of fluid is discussed in the following section. For δ^{18}O and more specifically for the euhedral quartz, the shift to more positive values can be explained by a buffering of the mineralizing fluid by the talc and chlorite due to a low fluid/rock ratio. The oxygen (and hydrogen) isotopic composition of the water in isotopic equilibrium with the euhedral quartz falls in, or is really close to, the chlorite and talc field (Figure 8) from the deposit. Thus, the H_2O uptake during the talc and chlorite formation is possibly at the origin of both the increase in chlorinity recorded in the quartz and calcite and the isotopic buffering of the fluid by the ore. Surprisingly, calcite, which is considered to be one of the last minerals to have precipitated, does not seem to be particularly affected by this process, suggesting that it formed under a higher fluid/rock ratio than quartz.

6.1.2. Evidence of Mixing between Primary Brines and Dilute Formation Waters. Chlorine proxies and stable isotope proxies provide consistent signatures indicating that the primary brines saturated with respect to halite are the brines that form the mineralizing fluid. However, the chlorinity ranges that include the lowest values close to 10% eq. NaCl, certain Cl/Br ratio values close to 650, and the general trend toward low δD values are all indications of partial mixing with other fluids.

Therefore, a mixing between more dilute waters may explain the slight scattering of certain values. Among the dilute waters, several endmembers may be considered: (i) recharge waters fed by meteoric inputs: such recharge waters may have leached the Triassic evaporites in some instances, which in turn could have resulted in an increase in Cl and are then the so-called secondary brines, (ii) (Albian) seawater, and (iii) formation waters which are known to have low δD values (up to -70‰) and oxygen isotopic compositions ranging between -10‰ and +10‰ [61]. These waters underwent various processes (e.g., a fluid-rock interaction implying chemical and isotopic modification, salt dissolution, and ion ultrafiltration) which altered the initial seawater composition [62]. In the geological context of this study, such waters are expected to have been hosted in the porosity of the overlying sediments. Based on the general trend of low δD values, the hypothesis of the mixing of primary brines with either secondary brines that have a meteoric origin or seawater is unlikely. Conversely, a mixing of evaporated seawater with formation waters should easily explain the low δD values and the slight salinity and Cl/Br data discrepancies.

6.1.3. From Dolomitization to Talc Formation. The dolomitization of the Devonian calcitic marbles is considered by Boulvais et al. [6] as belonging to a same and continuous water/rock interaction process that finally led to the formation of the talc. Our data support this interpretation and suggest that the whole magnesian metasomatic sequence (dolomitization-talcification-chloritization) results from the interaction between primary brines and rocks (calcitic marbles, pegmatites, and mica schists). Accordingly, the dolomitization of the calcitic marbles precedes the formation of the talc and chlorite. A significant supply of magnesium is therefore needed. As shown by Fontes and Matray [51], primary brines saturated with respect to halite are significantly enriched in magnesium, up to 50500 $mg{\cdot}L^{-1}$. We therefore propose that at least part of the magnesium needed for Mg-rich mineral formation may have been supplied by the evaporitic brine itself. This hypothesis could be consistent with the fact that, to date, the primary brines trapped in the deposit are depleted in magnesium [5].

As shown previously, a few fluid inclusions with lower salinities are also identified in the dolostones and show a large range of salinities from 18 to 28 wt% eq. NaCl and a few moderate saline fluid inclusions (Figure 5) reflecting mixing with formation waters. The changes in the degree of mixing between the dolomitization stage and the talc ore formation stage, in particular the increase in salinity and subsequently the cation concentration of the fluid (including the Mg^{2+} content), may possibly explain the changes in the main precipitated assemblages. It is also interesting to consider the role of CO_2 during the magnesian metasomatism. Boiron et al. [4, 5] identified brines with traces of N_2-$CO_2 \pm CH_4$ in the euhedral quartz from the geodes. The presence of a low-density volatile phase dominated by N_2, e.g., reflecting a rather low PCO_2 value, could be consistent with the results of experimental studies dealing with talc formation from dolostone. Indeed, Wan et al. [63] experimentally determined that the talc formation rate increases with increasing temperature and decreases with increasing PCO_2.

6.1.4. What about the Regional Circulation of Primary Brines? One regional sample, coming from a quartz-calcite vein system localized in the Devonian schists from Caussou, has recorded the circulation of similar brines as those studied in the Trimouns deposit, suggesting a regional extent of this fluid circulation. The average fluid salinities measured in in quartz and calcite from the vein are similar to those from Trimouns (25.6 wt% eq. NaCl) (Table 2). The plot of the Cl/Br ratio as a function of the Cl content (Figure 6) confirms that they are also primary brines saturated with respect to halite. In the Cl/Br vs. $\delta^{37}Cl$ plot (Table 1, Figure 7), the brines plot really close to the field of evaporated seawater. The δD values are also close to those corresponding to the Trimouns brines. However, the calculated $\delta^{18}O$ value pairs are significantly shifted with respect to the Trimouns data (Table 1, Figure 8). This difference could be due to (i) the involvement of another fluid, (ii) the use of an inappropriate fractionation coefficient between minerals and fluids, or (iii) the use of an inappropriate temperature (300°C) to calculate the $\delta^{18}O_{fluid}$ composition. Based on the similarity of the Cl/Br ratios, the salinities, and the $\delta^{37}Cl$ and δD values of the mineralizing fluid documented in Trimouns with the primary brine signature, it is unlikely that another source of fluid is involved. Different isotopic fractionation coefficients between quartz, calcite, and H_2O are available in the literature and are relatively consistent between them. The isotopic fractionation coefficient is between 8.2‰ and 6.9‰ for quartz and H_2O at 300°C [47, 64–68] and between 3.8‰ and 5.8‰ for calcite and H_2O at 300°C [48, 69–72]; an exception for this is provided by Kim and O'Neil [73] who predict a fractionation coefficient of -1 between calcite and H_2O at the same temperature. However, their slight differences cannot explain the large variation in the $\delta^{18}O_{fluid}$ values compared to the primary brine composition field (~10‰). If two minerals occur together, it is possible to postulate that they were in isotopic equilibrium when they formed from the mineralizing fluid and to calculate their temperature of formation using the $\Delta^{18}O_{quartz-calcite}$ value. In this way, temperatures of ~120°C are calculated using the fractionation coefficient between quartz and calcite given by Zheng [48], ~150°C using that provided by Clayton and Keiffer [74], and 280°C using the one cited by Sharp and Kirschner [66]. The calculated oxygen isotopic composition of the fluid (using [47, 48]) falls in (at 120°C) or close to (at 150°C) the range of the primary brines saturated with respect to halite (120°C → quartz: $\delta^{18}O = 5.2‰$ and calcite: $\delta^{18}O = 4.9‰$ and 150°C → quartz: $\delta^{18}O = 8‰$ and calcite: $\delta^{18}O = 7.6‰$). Even if this range of temperatures is rather somewhat low, the fluid documented in Caussou has very similar features to those of the mineralizing fluid and may reflect the cooling of the system at the end of the process.

6.2. Origin(s) of the Primary Brines

6.2.1. Primary Brines Expelled from the Triassic. The evaporitic Triassic was both widespread and distributed all along the Hercynian basement. Therefore, the involvement of Triassic brines in various geological contexts postdating the Trias evaporite formation is often inferred. Two main processes are often proposed. The first one consists of the expelling of the interstitial fluids (the salt porosity is up to several volume percentages, [75–78]) hosted in the evaporites, which are the residual fluids after seawater evaporation and salt precipitation. This type of brine is called a primary brine. The second one consists of the dissolution of salt by a less saline fluid generating the so-called secondary brines. Based on our results, we have demonstrated that the fluids at the origin of the deposit were primary brines saturated with respect to halite mixed with a minor amount of formation waters. We propose that such primary brines could have been expelled from the Triassic (Figure 9) during the Cretaceous by (i) Albian sediment overloading on the underlying Mesozoic rocks and/or (ii) the shearing of the Triassic levels induced by the gravity gliding of the Mesozoic series [79].

6.2.2. What about the Influence of Mantle Metasomatism? The recent literature underlines the fact that salt enrichment in fluids could originate from other processes, such as H_2O removal when forming hydrated minerals from anhydrous

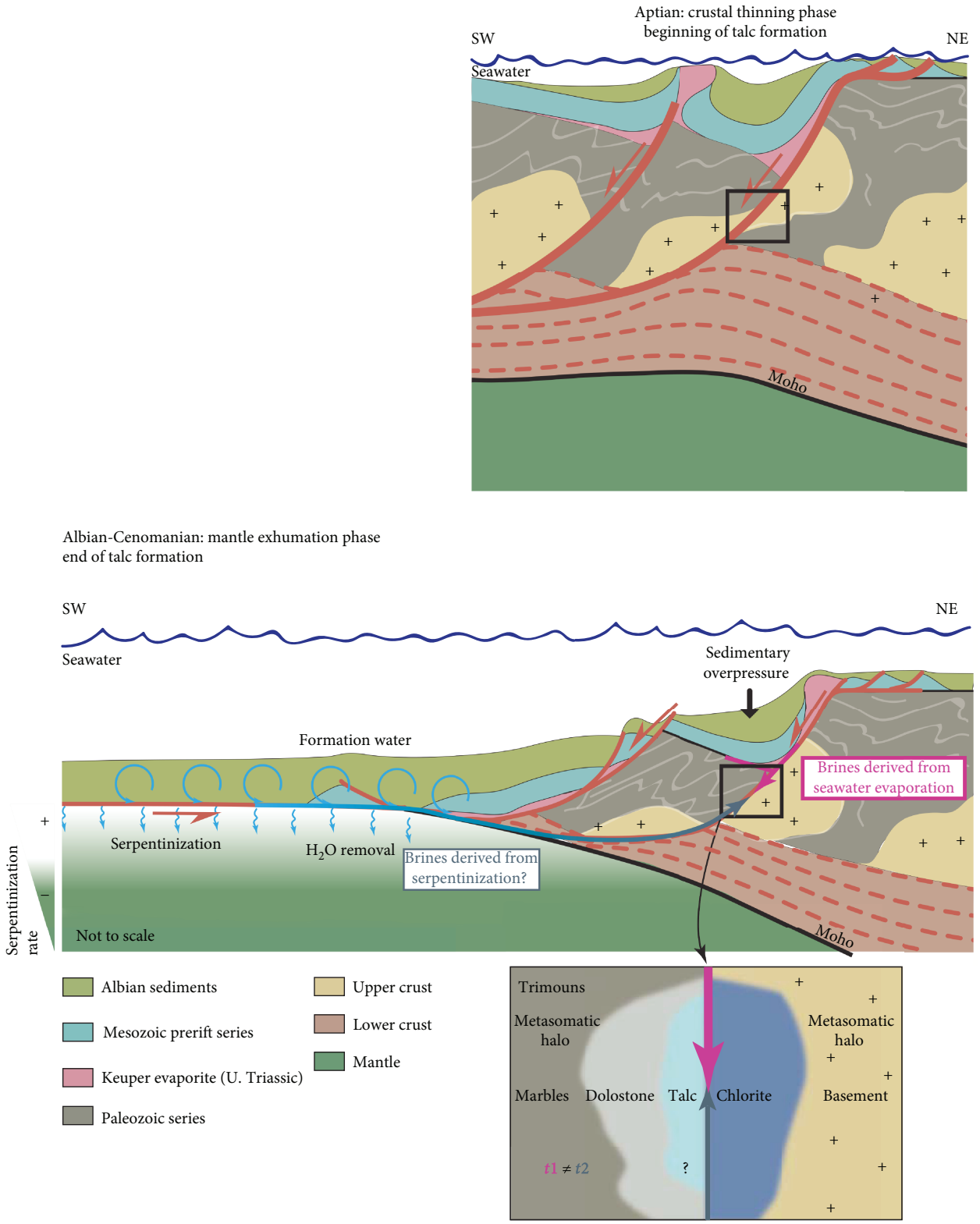

Figure 9: Conceptual cross-section of the North-Eastern Pyrenees region from Aptian to Turonian times with illustrations of (i) the fluid circulation model with two sources of primary brines. With respect to the hydrodynamics, the circulation of the two types of brines should have been temporally disconnected and (ii) the continuous interaction of these brines with the rocks leading to the formation of the whole magnesian metasomatic sequence (marbles → dolostones → talc; pegmatite + mica schists → chlorite ± talc). $t1 \neq t2$ represents the fact that the circulation of the brines derived from the seawater evaporation and derived from the serpentinization should have been temporally disconnected in the deposit.

ones ([39, 52, 54, 55, 58, 80]; Hovland et al., 2018). Carrying this idea a step further, Scribano et al. [81] suggested that the formation of a certain subseafloor giant salt deposit in deep marine basins may be genetically related to the serpentinization of ultramafic rocks. In the present context of passive margin hyperextension, mantle exhumation, and subsequent fluid circulation, several authors have already proposed that seawater-driven serpentinization may contribute to the transport of dissolved elements (Mg, Cr, and V; [82]). Recently, Corre et al. [83] suggested that such fluids circulated in the Saraillé Massif based on the Cr content of the chlorite localized in the detachment fault (average Cr content of 1.44 wt%). It is also interesting to note that in the latter case, these fluids are extremely saline with up to 27 wt% eq. NaCl.

Given the current proximity of the serpentinized peridotite bodies from the deposit (Figure 1), we suggest estimating the relevance of the oxygen and deuterium isotopic systems and chlorine proxies in order to test the hypothesis of mantle rock serpentinization and the subsequent generation of brines as a potential origin of the Trimouns deposit (Figure 9).

From an isotopic point of view, the generation of brine by seawater evaporation or serpentinization refers to two distinct processes leading to different fractionation effects. The first step consists of comparing the fluid isotopic composition documented here with the one expected for a fluid in isotopic equilibrium with serpentine. Unfortunately, the oxygen and deuterium isotopic compositions of the Pyrenean serpentines are not available. Despite this lack of data in the literature, we propose to consider the large range of modern oceanic serpentinites compiled by Pope et al. [84]. Considering a temperature of 300°C, it is possible to calculate the expected δD and δ^{18}O values of water in isotopic equilibrium with these serpentines [60]. As displayed in Figure 8, the large field of composition of such water overlaps the field of evaporated seawater and therefore the Trimouns data. This may indicate that stable isotopes cannot discriminate between the two processes.

Bonifacie et al. [85] and Barnes and Cisneros [86] measured the chlorine isotopic compositions of the oceanic serpentinites, which have δ^{37}Cl values ranging between -1.4‰ and +1.8‰. As explained by Bonifacie et al. [85], most serpentinites overlain by sediments show negative δ^{37}Cl values interpreted as resulting from the interaction with sediment pore waters [87] that have negative δ^{37}Cl values [45, 88–90]. This implies that serpentinization does not disturb the chlorine isotopic composition of the fluid, which keeps its negative signature. Consequently, in our case, the δ^{37}Cl value does not really help us to determine the origin of the brines.

As for the Cl/Br ratios, the chlorine behavior during the serpentinization of the peridotites is the only well constrained in the literature. The fresh oceanic lithosphere has low chlorine content (e.g., [91, 92]), whereas secondary minerals formed after a water-rock interaction can have high chlorine content, e.g., as serpentine ([93] and references herein). Consequently, serpentine can be considered as a "sink" for chlorine even if only a small amount of Cl can be incorporated at $T < 250$°C. With regard to the serpentinization-derived brine hypothesis, the interaction between the formation water (derived from Albian seawater) and the exhumed mantle should have led to a decreased chlorine content in the residual fluid. Thus, the expected Cl/Br ratio of the residual fluid should be lower than the initial one. Considering that the formation water probably was initially Albian seawater, the expected Cl/Br ratio of the formation water after the serpentinization (the residual fluid) should be lower than 650, a value that is consistent with our data. However, given that the behavior of the bromine during the serpentinization is poorly known, the expected Cl/Br composition of the residual fluid remains highly hypothetical.

7. New Insights into the Trimouns Magnesian Metasomatose Model

In this study, using complementary geochemical proxies (δD, δ^{18}O, δ^{37}Cl, and Cl/Br), we demonstrate that the formation of the talc-chlorite Trimouns deposit results from the interaction of primary brines saturated with respect to halite with the rocks lying on both sides of the fault located on the eastern border of the Saint Barthelemy Massif. Based on the chemical similarities of the fluid contained in the syn-deposit minerals (quartz and calcite) and antemineralization rocks (dolostones), we suggest that the whole magnesian metasomatic sequence (marble → dolostones → talc; pegmatite or mica schist → chlorite ± talc) results from successive pulses of primary brine saturated with respect to halite during a relatively long period of time (at least between 122 Ma and 96 Ma). We suggest that the evaporitic Triassic succession, which is both widespread and distributed on top of the Hercynian basement in the Pyrenees, is the main source of this fluid. In some cases, the chlorinity ranges that include the lowest values close to 10 wt% eq. NaCl, certain Cl/Br ratio values close to 650, and the general trend toward low δD values are all indications of partial mixing with lower salinity fluids such as formation waters hosted within the overlying sediments.

Given the particular geological context (hyperextension, mantle exhumation) in which the formation of the Trimouns deposit took place, we have also examined the possible influence of mantle metasomatism on the formation of primary brines. We conclude that, although our results are not entirely inconsistent with this hypothesis, the link with serpentinization is not demonstrated. Moreover, if brines derived from the serpentinization have been involved in the formation of the deposit, their circulation at the deposit level should be temporally disconnected from those of the brines derived from seawater evaporation. As suggested in the literature [54], it is difficult to invoke simultaneous downward and upward flows of the various fluids in order to explain the evidences for mixing in the deposit. From a geochemical point of view, additional studies are needed to clearly address the question of whether serpentinization can influence the formation of brines in the Pyrenees. First, a deuterium and oxygen isotopic survey of the Pyrenean serpentinites is required, and second, an equivalent survey focusing on the chlorine isotopic composition of the Pyrenean serpentinites would be also useful to test this hypothesis. Lastly, the

characterization of the magnesium isotopic composition of the dolostones, talc, chlorite, and serpentinites would provide some interesting insights. As has already been suggested by several authors, serpentinization is not isochemical [94–96] and magnesium should be transferred into the reacting fluid from peridotites during their alteration. This idea remains a matter of debate, and the comparing of the magnesium isotopic composition of the Pyrenean talc, chlorite, dolostones, and serpentinites could help to determine if the mantle provided part of the magnesium needed to form the deposit. However, to date, only evaporated seawater saturated with respect to halite is identified as the most likely source of magnesium.

Data Availability

The data used to support the findings of this study are available from the corresponding author upon request.

Conflicts of Interest

The authors declare that they have no conflicts of interest.

Acknowledgments

This work was financially and technically supported by Total S.A. We thank Thibaut Klein (Imerys Talc) for giving us access to the Luzenac mining site. Serge Fourcade, Philippe de Parseval, and Alexandre Boutin are warmly thanked for stimulating discussions on the field. Antonin Richard and Pierre Martz are warmly thanked for the fruitful discussions about brines in general. We also thank Yves Lagabrielle and Philippe Boulvais for the general discussions about the geological history of the Pyrenees. Sylvain Calassou is thanked for his scientific advices about the geometry of the Pyrenean hyperextended passive margin. Marina Kouadio and Frederic Diot are thanked for their technical support on the fluid inclusion study and ion chromatography, respectively. Enrique Gomez-Rivas is thanked for his constructive review that helped the authors improve the clarity of the manuscript.

References

[1] P. Boulvais, G. Ruffet, J. Cornichet, and M. Mermet, "Cretaceous albitization and dequartzification of Hercynian peraluminous granite in the Salvezines Massif (French Pyrénées)," *Lithos*, vol. 93, no. 1-2, pp. 89–106, 2007.

[2] C. Clerc and Y. Lagabrielle, "Thermal control on the modes of crustal thinning leading to mantle exhumation: insights from the Cretaceous Pyrenean hot paleomargins," *Tectonics*, vol. 33, no. 7, pp. 1340–1359, 2014.

[3] P. Monchoux, *Les lherzolites pyrénéenes. Contribution à l'étude de leur minéralogie, de leur genèse et de leurs transformations, Th'se d'état*, Univ. Toulouse, 1970.

[4] M.-C. Boiron, P. Boulvais, M. Cathelineau, D. Banks, N. Calvayrac, and G. Hubert, *Fluid Circulation at the Origin of the Trimouns Talc Deposit (Pyrenees, France)*, ECROFI XVIII, Siena, 2005.

[5] M.-C. Boiron, M. Cathelineau, J. Dubessy, C. Fabre, P. Boulvais, and D. Banks, "Na Ca-Mg rich brines and talc formation in the giant talc deposit of Trimouns (Pyrénées): fluid inclusion chemistry and stable isotope study," in *European Current Research on Fluid Inclusions (ECROFI-XIX)*, p. 1, University of Bern, Switzerland, 2007.

[6] P. Boulvais, P. de Parseval, A. D'Hulst, and P. Paris, "Carbonate alteration associated with talc-chlorite mineralization in the Eastern Pyrenees, with emphasis on the St. Barthelemy Massif," *Mineralogy and Petrology*, vol. 88, no. 3-4, pp. 499–526, 2006.

[7] A. Boutin, *2tude des conditions de formation du gisement de talc-chlorite de Trimouns, [Ph. D. thesis]*, Univesrité de Toulouse, 2016.

[8] B. Moine, J.-P. Fortuné, P. Moreau, and F. Viguier, "Comparative mineralogy, geochemistry, and conditions of formation of two metasomatic talc and chlorite deposits; Trimouns (Pyrenees, France) and Rabenwald (Eastern Alps, Austria)," *Economic Geology*, vol. 84, no. 5, pp. 1398–1416, 1989.

[9] S. Renard, J. Pironon, J. Sterpenich, C. Carpentier, M. Lescanne, and E. C. Gaucher, "Diagenesis in Mesozoic carbonate rocks in the North Pyrénées (France) from mineralogy and fluid inclusion analysis: example of Rousse reservoir and caprock," *Chemical Geology*, vol. 508, pp. 30–46, 2018.

[10] A. Boutin, M. de Saint Blanquat, M. Poujol et al., "Succession of Permian and Mesozoic metasomatic events in the Eastern Pyrenees with emphasis on the Trimouns talc–chlorite deposit," *International Journal of Earth Sciences*, vol. 105, no. 3, pp. 747–770, 2016.

[11] O. Dauteuil and L. E. Ricou, "Hot-fluid circulation as an origin for the North Pyrenean Cretaceous metamorphism," *Geodinamica Acta*, vol. 3, no. 3, pp. 237–249, 1989.

[12] S. Fallourd, M. Poujol, P. Boulvais, J.-L. Paquette, M. de Saint Blanquat, and P. Rémy, "In situ LA-ICP-MS U–Pb titanite dating of Na–Ca metasomatism in orogenic belts: the North Pyrenean example," *International Journal of Earth Sciences*, vol. 103, no. 3, pp. 667–682, 2014.

[13] M. Poujol, P. Boulvais, and J. Kosler, "Regional-scale Cretaceous albitization in the Pyrenees: evidence from in situ U–Th–Pb dating of monazite, titanite and zircon," *Journal of the Geological Society*, vol. 167, no. 4, pp. 751–767, 2010.

[14] U. Schärer, P. de Parseval, M. Polvé, and M. de Saint Blanquat, "Formation of the Trimouns talc chlorite deposit from persistent hydrothermal activity between 112 and 97 Ma," *Terra Nova*, vol. 11, no. 1, pp. 30–37, 1999.

[15] Y. Lagabrielle and J.-L. Bodinier, "Submarine reworking of exhumed subcontinental mantle rocks: field evidence from the Lherz peridotites, French Pyrenees," *Terra Nova*, vol. 20, no. 1, pp. 11–21, 2008.

[16] J. M. Golberg and A. F. Leyreloup, "High temperature-low pressure Cretaceous metamorphism related to crustal thinning (Eastern North Pyrenean Zone, France)," *Contributions to Mineralogy and Petrology*, vol. 104, no. 2, pp. 194–207, 1990.

[17] J.-M. Golberg and H. Maluski, "Données nouvelles et mise au point sur l'âge du métamorphisme pyrénéen," *Comptes Rendus de l'académie des Sciences de Paris*, vol. 306, pp. 429–435, 1988.

[18] J.-M. Golberg, *Le métamorphisme mésozoïque dans la partie orientale des Pyrénées: relation avec l'évolution de la chaîne au Crétacé, [M.S. thesis]*, Montpellier II, 1987.

[19] D. Vielzeuf and J. Kornprobst, "Crustal splitting and the emplacement of Pyrenean lherzolites and granulites," *Earth and Planetary Science Letters*, vol. 67, no. 1, pp. 87–96, 1984.

[20] W. L. Pohl, *Economic Geology Principles and Practice: Metals, Minerals, Coal and Hydrocarbons – Introduction to Formation*

and Sustainable Exploitation of Mineral Deposits, Wiley-Blackwell, Oxford, UK, 2011.

[21] P. Choukroune, X. Le Pichon, M. Seguret, and J.-C. Sibuet, "Bay of Biscay and Pyrenees," *Earth and Planetary Science Letters*, vol. 18, no. 1, pp. 109–118, 1973.

[22] P. Choukroune and M. Mattauer, "Tectonique des plaques et Pyrenees; sur le fonctionnement de la faille transformante nord-pyreneenne; comparaisons avec des modeles actuels," *Bulletin de la Societe Geologique de France*, vol. S7-XX, no. 5, pp. 689–700, 1978.

[23] X. Le Pichon, J. Bonnin, and J.-C. Sibuet, "La faille nord-pyrénéenne: faille transformante liée à l'ouverture du golfe de Gascogne," *Comptes Rendus Hebdomadaires des séances de l'académie des Sciences Série D*, vol. 271, pp. 1941–1944, 1970.

[24] J.-L. Olivet, "La cinématique de la plaque ibérique," *Bulletin des Centres de Recherches Exploration-Production Elf-Aquitaine*, vol. 20, pp. 131–195, 1996.

[25] M. de Saint Blanquat, M. Brunel, and M. Mattauer, "Les zones de cisaillements du massif Nord Pyrénéen du Saint Barthélémy, témoins probables de l'extension crustale d'âge crétacé," *Comptes Rendus de l'académie des Sciences de Paris*, vol. 303, pp. 1339–1344, 1986.

[26] F. Albarède and A. Michard-Vitrac, "Age and significance of the North Pyrenean metamorphism," *Earth and Planetary Science Letters*, vol. 40, no. 3, pp. 327–332, 1978.

[27] C. Clerc, A. Lahfid, P. Monié et al., "High-temperature metamorphism during extreme thinning of the continental crust: a reappraisal of the North Pyrenean passive paleomargin," *Solid Earth*, vol. 6, no. 2, pp. 643–668, 2015.

[28] R. Montigny, B. Azambre, M. Rossy, and R. Thuizat, "K-Ar study of Cretaceous magmatism and metamorphism in the Pyrenees: age and length of rotation of the Iberian Peninsula," *Tectonophysics*, vol. 129, no. 1-4, pp. 257–273, 1986.

[29] P. De Parseval, *Étude minéralogique et géochimique du gisement de talc et chlorite de Trimouns, [Ph. D. thesis]*, Université de Toulouse III, 1992.

[30] P. De Parseval, F. Fontan, and T. Agouy, "Composition chimique des minéraux de terres rares de Trimouns (Ariège, France)," *Comptes Rendus de l'académie des Sciences de Paris*, vol. 625, no. 630, p. 324, 1997.

[31] P. De Parseval, S. Jiang, F. Fontan, F. Martins, and J. Freeet, "Geology and ore genesis of the Trimouns talc chlorite ore deposit," *Acta Petrologica Sinica*, vol. 20, pp. 877–886, 2004.

[32] M. de Saint Blanquat, *La faille normale ductile du massif du Saint Barthélémy (age et signification de l'extension crustale dans la Zone Nord Pyrénéenne), [Ph.D. thesis]*, Université de Montpellier II, France, 1989.

[33] M. de Saint Blanquat, J. M. Lardeaux, and M. Brunel, "Petrological arguments for high-temperature extensional deformation in the Pyrenean Variscan crust (Saint Barthélémy Massif, Ariège, France)," *Tectonophysics*, vol. 177, no. 1-3, pp. 245–262, 1990.

[34] M. Leisen, M.-C. Boiron, A. Richard, and J. Dubessy, "Determination of Cl and Br concentrations in individual fluid inclusions by combining microthermometry and LA-ICPMS analysis: implications for the origin of salinity in crustal fluids," *Chemical Geology*, vol. 330-331, pp. 197–206, 2012.

[35] J. Dubessy, T. Lhomme, M. C. Boiron, and F. Rull, "Determination of chlorinity in aqueous fluids using Raman spectroscopy of the stretching band of water at room temperature: application to fluid inclusions," *Applied Spectroscopy*, vol. 56, no. 1, pp. 99–106, 2002.

[36] M.-C. Caumon, J. Dubessy, P. Robert, and A. Tarantola, "Fused-silica capillary capsules (FSCCs) as reference synthetic aqueous fluid inclusions to determine chlorinity by Raman spectroscopy," *European Journal of Mineralogy*, vol. 25, no. 5, pp. 755–763, 2013.

[37] D. A. Banks and B. W. D. Yardley, "Crush-leach analysis of fluid inclusions in small natural and synthetic samples," *Geochimica et Cosmochimica Acta*, vol. 56, no. 1, pp. 245–248, 1992.

[38] D. A. Banks, G. Guiliani, B. W. D. Yardley, and A. Cheilletz, "Emerald mineralisation in Colombia: fluid chemistry and the role of brine mixing," *Mineralium Deposita*, vol. 35, no. 8, pp. 699–713, 2000.

[39] S. A. Gleeson, B. W. D. Yardley, I. A. Munz, and A. J. Boyce, "Infiltration of basinal fluids into high-grade basement, South Norway: sources and behaviour of waters and brines," *Geofluids*, vol. 3, no. 1, 48 pages, 2003.

[40] M. Bonifacie, J.-L. Charlou, N. Jendrzejewski, P. Agrinier, and J.-P. Donval, "Chlorine isotopic compositions of high temperature hydrothermal vent fluids over ridge axes," *Chemical Geology*, vol. 221, no. 3-4, pp. 279–288, 2005.

[41] M. Bonifacie, C. Monnin, N. Jendrzejewski, P. Agrinier, and M. Javoy, "Chlorine stable isotopic composition of basement fluids of the eastern flank of the Juan de Fuca Ridge (ODP Leg 168)," *Earth and Planetary Science Letters*, vol. 260, no. 1-2, pp. 10–22, 2007.

[42] H. G. M. Eggenkamp, *$d^{37}Cl$, the geochemistry of chlorine isotopes, [Ph. D. thesis]*, Utrecht University, 1994.

[43] A. Godon, N. Jendrzejewski, H. G. M. Eggenkamp et al., "A cross-calibration of chlorine isotopic measurements and suitability of seawater as the international reference material," *Chemical Geology*, vol. 207, no. 1-2, pp. 1–12, 2004.

[44] T. Giunta, M. Ader, M. Bonifacie, P. Agrinier, and M. Coleman, "Pre-concentration of chloride in dilute water-samples for precise δ^{37}Cl determination using a strong ion-exchange resin: application to rainwaters," *Chemical Geology*, vol. 413, pp. 86–93, 2015.

[45] A. Godon, N. Jendrzejewski, M. Castrec-Rouelle et al., "Origin and evolution of fluids from mud volcanoes in the Barbados accretionary complex," *Geochimica et Cosmochimica Acta*, vol. 68, no. 9, pp. 2153–2165, 2004.

[46] R. N. Clayton and T. K. Mayeda, "The use of bromine pentafluoride in the extraction of oxygen from oxides and silicates for isotopic analysis," *Geochimica et Cosmochimica Acta*, vol. 27, no. 1, pp. 43–52, 1963.

[47] Y.-F. Zheng, "Calculation of oxygen isotope fractionation in anhydrous silicate minerals," *Geochimica et Cosmochimica Acta*, vol. 57, no. 5, pp. 1079–1091, 1993.

[48] Y. F. Zheng, "Oxygen isotope fractionation in carbonate and sulfate minerals," *Geochemical Journal*, vol. 33, no. 2, pp. 109–126, 1999.

[49] C. J. Eastoe, A. Long, and L. P. Knauth, "Stable chlorine isotopes in the Palo Duro Basin, Texas: evidence for preservation of Permian evaporite brines," *Geochimica et Cosmochimica Acta*, vol. 63, no. 9, pp. 1375–1382, 1999.

[50] H. G. M. Eggenkamp, R. Kreulen, and A. F. Koster Van Groos, "Chlorine stable isotope fractionation in evaporites," *Geochimica et Cosmochimica Acta*, vol. 59, no. 24, pp. 5169–5175, 1995.

[51] J. C. Fontes and J. M. Matray, "Geochemistry and origin of formation brines from the Paris Basin, France: 1. Brines associated with Triassic salts," *Chemical Geology*, vol. 109, no. 1-4, pp. 149–175, 1993.

[52] P. Martz, J. Mercadier, M. Cathelineau et al., "Formation of U-rich mineralizing fluids through basinal brine migration within basement-hosted shear zones: a large-scale study of the fluid chemistry around the unconformity-related Cigar Lake U deposit (Saskatchewan, Canada)," *Chemical Geology*, vol. 508, pp. 116–143, 2018.

[53] A. Richard, D. A. Banks, J. Mercadier, M. C. Boiron, M. Cuney, and M. Cathelineau, "An evaporated seawater origin for the ore-forming brines in unconformity-related uranium deposits (Athabasca Basin, Canada): Cl/Br and δ^{37}Cl analysis of fluid inclusions," *Geochimica et Cosmochimica Acta*, vol. 75, no. 10, pp. 2792–2810, 2011.

[54] P. D. Bons, T. Fusswinkel, E. Gomez-Rivas, G. Markl, T. Wagner, and B. Walter, "Fluid mixing from below in unconformity-related hydrothermal ore deposits," *Geology*, vol. 42, no. 12, pp. 1035–984 1038, 2014.

[55] B. F. Walter, M. Burisch, and G. Markl, "Long-term chemical evolution and modification of continental basement brines – a field study from the Schwarzwald, SW Germany," *Geofluids*, vol. 16, no. 3, 623 pages, 2016.

[56] W. Holser, "Chapter 9. Trace elements and isotopes in evaporites," in *Marine Minerals*, R. G. Burns, Ed., vol. 6 of Reviews in Mineralogy, pp. 295–346, De Gruyter, Berlin, Boston, 1979.

[57] L. P. Knauth and M. A. Beeunas, "Isotope geochemistry of fluid inclusions in Permian halite with implications for the isotopic history of ocean water and the origin of saline formation waters," *Geochimica et Cosmochimica Acta*, vol. 50, no. 3, pp. 419–433, 1986.

[58] A. Richard, P. Boulvais, J. Mercadier et al., "From evaporated seawater to uranium-mineralizing brines: isotopic and trace element study of quartz–dolomite veins in the Athabasca system," *Geochimica et Cosmochimica Acta*, vol. 113, pp. 38–59, 2013.

[59] Y.-F. Zheng, "Calculation of oxygen isotope fractionation in hydroxyl-bearing silicates," *Earth and Planetary Science Letters*, vol. 120, no. 3-4, pp. 247–263, 1993.

[60] P. J. Saccocia, J. S. Seewald, and W. C. Shanks Iii, "Oxygen and hydrogen isotope fractionation in serpentine–water and talc–water systems from 250 to 450 ˚C, 50 MPa," *Geochimica et Cosmochimica Acta*, vol. 73, no. 22, pp. 6789–6804, 2009.

[61] S. M. F. Sheppard, "Stable isotope variations in natural waters," in *Stable Isotopes in High Temperature Geologic Processes*, J. W. Valley, H. P. Taylor, and J. R. O'Neil, Eds., vol. 16 of Review in Mineralogy and Geochemistry, pp. 319–372, 1986.

[62] H. G. M. Eggenkamp, *The Geochemistry of Stable Chlorine and Bromine Isotopes*, Springer, 2014.

[63] Y. Wan, X. Wang, I.-M. Chou, W. Hu, Y. Zhang, and X. Wang, "An experimental study of the formation of talc through $CaMg(CO3)_2$–SiO_2–H_2O interaction at 100-200˚C and vapor-saturation pressures," *Geofluids*, vol. 2017, Article ID 3942826, 14 pages, 2017.

[64] Y. Matsuhisa, J. R. Goldsmith, and R. N. Clayton, "Oxygen isotopic fractionation in the system quartz-albite-anorthite-water," *Geochimica et Cosmochimica Acta*, vol. 43, no. 7, pp. 1131–1140, 1979.

[65] Z. D. Sharp, J. A. Gibbons, O. Maltsev et al., "A calibration of the triple oxygen isotope fractionation in the SiO_2–H_2O system and applications to natural samples," *Geochimica et Cosmochimica Acta*, vol. 186, pp. 105–119, 2016.

[66] Z. D. Sharp and D. L. Kirschner, "Quartz-calcite oxygen isotope thermometry: a calibration based on natural isotopic variations," *Geochimica et Cosmochimica Acta*, vol. 58, no. 20, pp. 4491–4501, 1994.

[67] Y. Shiro and H. Sakai, "Calculation of the reduced partition function ratios of α-, β-quartzs and calcite," *Bulletin of the Chemical Society of Japan*, vol. 45, no. 8, pp. 2355–2359, 1972.

[68] L.-G. Zhang, J.-X. Liu, H. B. Zhou, and Z.-S. Chen, "Oxygen isotope fractionation in the quartz-water-salt system," *Economic Geology*, vol. 84, no. 6, pp. 1643–1650, 1989.

[69] S. I. Golyshev, N. L. Padalko, and S. A. Pechenkin, "Fractionation of stable oxygen and carbon isotopes in carbonate systems," *Geochemistry International*, vol. 18, pp. 85–99, 1981.

[70] G. X. Hu and R. N. Clayton, "Oxygen isotope salt effects at high pressure and high temperature and the calibration of oxygen isotope geothermometers," *Geochimica et Cosmochimica Acta*, vol. 67, no. 17, pp. 3227–3246, 2003.

[71] J. Horita, "Oxygen and carbon isotope fractionation in the system dolomite–water–CO_2 to elevated temperatures," *Geochimica et Cosmochimica Acta*, vol. 129, pp. 111–124, 2014.

[72] J. R. O'Neil, R. N. Clayton, and T. K. Mayeda, "Oxygen isotope fractionation in divalent metal carbonates," *The Journal of Chemical Physics*, vol. 51, no. 12, pp. 5547–5558, 1969, NOTE: the equations are recalculated by Freidman and O'Neil (1977) to account for a different value of the H_2O-CO_2 fractionation.

[73] S.-T. Kim and J. R. O'Neil, "Equilibrium and nonequilibrium oxygen isotope effects in synthetic carbonates," *Geochimica et Cosmochimica Acta*, vol. 61, no. 16, pp. 3461–3475, 1997.

[74] R. N. Clayton and S. W. Keiffer, "Oxygen isotopic thermometer calibrations," in *Stable Isotope Geochemistry: A Tribute to Samuel Epstein*, H. P. Taylor, J. R. O'Neil, and I. R. Kaplan, Eds., pp. 3–10, The Geochemical Society, 1991, Special Publication no.3.

[75] M. Cathelineau, M.-C. Boiron, S. Fourcade et al., "A major Late Jurassic fluid event at the basin/basement unconformity in western France: ^{40}Ar/^{39}Ar and K–Ar dating, fluid chemistry, and related geodynamic context," *Chemical Geology*, vol. 322-323, pp. 99–120, 2012.

[76] C. De Las Cuevas, "Pore structure characterization in rock salt," *Engineering Geology*, vol. 47, no. 1-2, pp. 17–30, 1997.

[77] R. Sieland, "Hydraulic investigations of the Salar de Uyuni, *Bolivia*," *Freiberg Online Geology*, vol. 37, p. 208, 2014.

[78] N. Thiemeyer, M. Pusch, J. Hammer, and G. Zulauf, "Quantification and 3D visualisation of pore space in Gorleben rock salt: constraints from CT imaging and microfabrics Quantifizierung und 3D-Visualisierung des Porenraumes in Gorleben-Steinsalz: Ergebnisse computertomografischer und mikrostruktureller Untersuchungen," *Zeitschrift der Deutschen Gesellschaft für Geowissenschaften*, vol. 165, no. 1, pp. 15–25, 2014.

[79] Y. Lagabrielle, P. Labaume, and M. de Saint Blanquat, "Mantle exhumation, crustal denudation, and gravity tectonics during Cretaceous rifting in the Pyrenean realm (SW Europe): insights from the geological setting of the lherzolite bodies," *Tectonics*, vol. 29, no. 4, 2010.

[80] I. Stober and K. Bucher, "Fluid sinks within the earth's crust," *Geofluids*, vol. 4, no. 2, 151 pages, 2004.

[81] V. Scribano, S. Carbone, F. C. Manuella, M. Hovland, H. Rueslatten, and H.-K. Johnsen, "Origin of salt giants in

abyssal serpentinite systems," *International Journal of Earth Sciences*, vol. 106, no. 7, pp. 2595–2608, 2017.

[82] V. H. G. Pinto, G. Manatschal, A. M. Karpoff, and A. Viana, "Tracing mantle-reacted fluids in magma-poor rifted margins: the example of Alpine Tethyan rifted margins," *Geochemistry, Geophysics, Geosystems*, vol. 16, no. 9, pp. 3271–3308, 2015.

[83] B. Corre, P. Boulvais, M.-C. Boiron, Y. Lagabrielle, L. Marasi, and C. Clerc, "Fluid circulations in response to mantle exhumation at the passive margin setting in the North Pyrenean Zone, France," *Mineralogy and Petrology*, vol. 112, no. 5, pp. 647–670, 2018.

[84] E. C. Pope, D. K. Bird, and M. T. Rosing, "Isotope composition and volume of Earth's early oceans," *Proceedings of the National Academy of Sciences of the United States of America*, vol. 109, no. 12, pp. 4371–4376, 2012.

[85] M. Bonifacie, V. Busigny, C. Mével et al., "Chlorine isotopic composition in seafloor serpentinites and high-pressure metaperidotites. Insights into oceanic serpentinization and subduction processes," *Geochemica et Cosmochimica Acta*, vol. 72, no. 1, pp. 126–139, 2008.

[86] J. D. Barnes and M. Cisneros, "Mineralogical control on the chlorine isotope composition of altered oceanic crust," *Chemical Geology*, vol. 326-327, pp. 51–60, 2012.

[87] J. D. Barnes and Z. D. Sharp, "A chlorine isotope study of DSDP/ODP serpentinized ultramafic rocks: insights into the serpentinization process," *Chemical Geology*, vol. 228, no. 4, pp. 246–265, 2006.

[88] B. Ransom, A. J. Spivack, and M. Kastner, "Stable Cl isotopes in subduction-zone pore waters: implications for fluid-rock reactions and the cycling of chlorine," *Geology*, vol. 23, no. 8, pp. 715–718, 1995.

[89] A. J. Spivack, M. Kastner, and B. Ransom, "Elemental and isotopic chloride geochemistry and fluid flow in the Nankai Trough," *Geophysical Research Letters*, vol. 29, no. 14, 2002.

[90] M. A. Stewart and A. J. Spivack, "The stable-chlorine isotope compositions of natural and anthropogenic materials," *Reviews in Mineralogy & Geochemistry*, vol. 55, no. 1, pp. 231–254, 2004.

[91] A. Jambon, B. Duruelle, G. Dreibus, and F. Pineau, "Chlorine and bromine abundance in MORB: the contrasting behaviour of the Mid-Atlantic Ridge and East Pacific Rise and implications for chlorine geodynamic cycle," *Earth and Planetary Science Letters*, vol. 126, pp. 101–117, 1995.

[92] P. J. Michael and W. C. Cornell, "Influence of spreading rate and magma supply on crystallization and assimilation beneath mid-ocean ridges: evidence from chlorine and major element chemistry of mid-ocean ridge basalts," *Journal of Geophysical Research: Solid Earth*, vol. 103, no. B8, pp. 18325–18356, 1998.

[93] C. Mével, "Serpentinization of abyssal peridotites at mid-ocean ridges," *Comptes Rendus Geoscience*, vol. 335, no. 10-11, pp. 825–852, 2003.

[94] B. Malvoisin, "Mass transfer in the oceanic lithosphere: serpentinization is not isochemical," *Earth and Planetary Science Letters*, vol. 430, pp. 75–85, 2015.

[95] V. H. Pinto, *Linking tectonic evolution with fluid history in hyperextended rifted margins: examples from the fossil Alpine and Pyrenean rift systems, and the present-day Iberia rifted margin, [Ph. D tthesis]*, Université de Strasbourg, 2014.

[96] J. E. Snow and H. J. B. Dick, "Pervasive magnesium loss by marine weathering of peridotite," *Geochimica et Cosmochimica Acta*, vol. 59, no. 20, pp. 4219–4235, 1995.